

Angular correlation of cosmic neutrinos with ultrahigh-energy cosmic rays and implications for their sources

Reetanjali Moharana and Soebur Razzaque

Department of Physics, University of Johannesburg,
P. O. Box 524, Auckland Park 2006, South Africa

E-mail: reetanjalin@uj.ac.za, srazzaque@uj.ac.za

Abstract. Cosmic neutrino events detected by the IceCube Neutrino Observatory with energy $\gtrsim 30$ TeV have poor angular resolutions to reveal their origin. Ultrahigh-energy cosmic rays (UHECRs), with better angular resolutions at > 60 EeV energies, can be used to check if the same astrophysical sources are responsible for producing both neutrinos and UHECRs. We test this hypothesis, with statistical methods which emphasize invariant quantities, by using data from the Pierre Auger Observatory, Telescope Array and past cosmic-ray experiments. We find that the arrival directions of the cosmic neutrinos are correlated with ≥ 100 EeV UHECR arrival directions at confidence level $\approx 90\%$. The strength of the correlation decreases with decreasing UHECR energy and no correlation exists at energy ~ 60 EeV. A search in astrophysical databases within 3° of the arrival directions of UHECRs with energy ≥ 100 EeV, that are correlated with the IceCube cosmic neutrinos, resulted in 18 sources from the *Swift*-BAT X-ray catalog with redshift $z \leq 0.06$. We also found 3 objects in the Kühn catalog of radio sources using the same criteria. The sources are dominantly Seyfert galaxies with Cygnus A being the most prominent member. We calculate the required neutrino and UHECR fluxes to produce the observed correlated events, and estimate the corresponding neutrino luminosity (25 TeV–2.2 PeV) and cosmic-ray luminosity (500 TeV–180 EeV), assuming the sources are the ones we found in the *Swift*-BAT and Kühn catalogs. We compare these luminosities with the X-ray luminosity of the corresponding sources and discuss possibilities of accelerating protons to $\gtrsim 100$ EeV and produce neutrinos in these sources.

Contents

1	Introduction	1
2	IceCube neutrino events and UHECR data	2
3	Statistical method and data analyses	5
4	Results	6
4.1	Correlations between neutrinos and UHECRs	6
4.2	Energy calibrated events	11
4.3	Astrophysical source search	12
4.4	Neutrino and UHECR luminosities for correlated events	14
5	Discussion and Outlook	18

1 Introduction

The IceCube Neutrino Observatory, the world’s largest neutrino detector, has recently published neutrino events collected over 3-year period with energy in the ~ 30 TeV–2 PeV range [1]. Shower events, most likely due to ν_e or ν_τ charge current νN interactions, dominate the event list (28 including 3 events with 1–2 PeV energy) while track events, most likely due to ν_μ charge current νN interactions, constitute the rest. Among a total of 37 events about 15 could be due to atmospheric neutrino ($6.6_{-1.6}^{+5.9}$) and muon (8.4 ± 4.2) backgrounds. A background-only origin of all 37 events has been rejected at $5.7\text{-}\sigma$ level [1]. Therefore a cosmic origin of a number of neutrino events is robust. The track events have on average $\sim 1^\circ$ angular resolution, but the dominant, shower events have much poorer angular resolution, $\sim 15^\circ$ on average [1], thus making them unsuitable for astronomy.

Meanwhile the Pierre Auger Observatory (PAO) [2] and the Telescope Array (TA) [3], two of the world’s largest operating cosmic-ray detectors, have recently released UHECR data collected over more than 10-year and 5-year periods, respectively. Together they have detected 16 events (6 by PAO [2] and 10 by TA [3]) with energies $\gtrsim 100$ EeV. The total publicly available $\gtrsim 100$ EeV events including past experiments is 33. While lower-energy cosmic ray arrival directions are scrambled by the Galactic and intergalactic magnetic fields, at $\gtrsim 60$ EeV energies the arrival directions of UHECRs tend to be much better correlated with their source directions and astronomy with charged particles could be realized [4]. Few degree angular resolution can be achieved at these energies, which is much better than the IceCube neutrino shower events and is comparable to the neutrino track events.

The astrophysical sources of UHECRs with energy $\gtrsim 40$ EeV need to be located within the so-called GZK volume [5, 6] in order to avoid serious attenuation of flux from them due to interactions of UHECRs with photons from cosmic microwave background (CMB) and extragalactic background light (EBL). The astrophysical sources of neutrinos, on the other hand, can be located at large distances and still be detected provided their luminosity is sufficiently high. However, because of weakly interacting nature of neutrinos and limiting luminosity of astrophysical sources, only nearby neutrino sources can be identified, thus making neutrino astronomy possible.

We explore here a possibility that both UHECRs and IceCube cosmic neutrino events are produced by the same astrophysical sources within the GZK volume. Since widely accepted Fermi acceleration mechanism of cosmic rays at the sources take place over a large energy range, it is natural that the same sources produce $\gtrsim 1$ PeV cosmic rays, required to produce cosmic neutrinos observed with energies down to ~ 30 TeV, and UHECRs with energy ≥ 40 EeV. We employ invariant statistical method [7, 8], independent of coordinate systems, in order to study angular correlation between cosmic neutrinos and UHECRs. As far we know, this is the first attempt to quantify such a correlation between the IceCube neutrino and UHECR data sets. Existence of such a correlation can provide clues to the origin of both cosmic neutrinos and UHECRs. We search for astrophysical sources within the angular errors of UHECRs which are correlated with the neutrino events in order to shed lights on their plausible, common origins. Finally we calculate required neutrino and cosmic-ray luminosities for the sources to produce observed events, and compare these luminosities with their observed X-ray and radio luminosities to check if they are viable sources of both UHECRs and cosmic neutrinos.

The organization of this paper is the following. We describe neutrino and UHECR data that we use in section 2 and our statistical method in section 3. The results of our correlation study and source search along the directions of the correlated events are given in section 4. Section 4 also includes calculation of neutrino and cosmic-ray luminosities of the correlated sources from respective fluxes derived using data. We discuss our results and implications of our findings in section 5.

2 IceCube neutrino events and UHECR data

We consider 35 IceCube neutrino events, collected over 988 days in the ~ 30 TeV–2 PeV range, from ref. [1] to study angular correlation with UHECRs. Two track events (event numbers 28 and 32) are coincident hits in the IceTop surface array and are almost certainly a pair of atmospheric muon background events [1]. Therefore we excluded them from our analysis. Figure 1 shows sky maps of 35 events in equatorial coordinates with reported angular errors. The majority (26) of the events have arrival directions in the southern sky. Among the 9 northern hemisphere events, only 1 is at a declination $Dec > 41^\circ$ which happens to be a shower event [1]. The angular resolutions of the track events are $\lesssim 1.4^\circ$ and those of the shower events vary between 6.6° and 46.3° . Figure 2 shows sky maps in Galactic coordinates.

Figures 1 and 2 also show sky maps of available UHECR data with energies ≥ 100 EeV (top panel) and ≥ 40 EeV (bottom panel). The PAO and TA collaborations have published data with energies above 52 EeV (231 events) [2] and 57 EeV (72 events) [3], respectively. Note that the PAO and TA are located in the southern and northern hemisphere, respectively, covering a declination range of $-90^\circ \leq Dec \leq 45^\circ$ [2] and $-10^\circ \leq Dec \leq 90^\circ$ [3]. The angular resolutions for the PAO events with energy > 10 EeV is $< 0.9^\circ$ [9] while for the TA events with energy > 57 EeV it is between 1.0° and 1.7° [3]. Note that the ≥ 40 EeV data sample is incomplete. Only the AGASA experiment has published data above 40 EeV (40 events) covering a declination range $-10^\circ \leq Dec \leq 90^\circ$ and with angular resolution $< 2^\circ$ [12]. Only ≥ 100 EeV data are available from the other past experiments: Haverah Park [10, 11], Yakutsk [10], Volcano Ranch [10] and Fly’s eye [10]. Note that these were all northern hemisphere experiments. We could not include 13 events with energy > 56 EeV from the HiRes experiment as the energies of the individual events are not available [13].

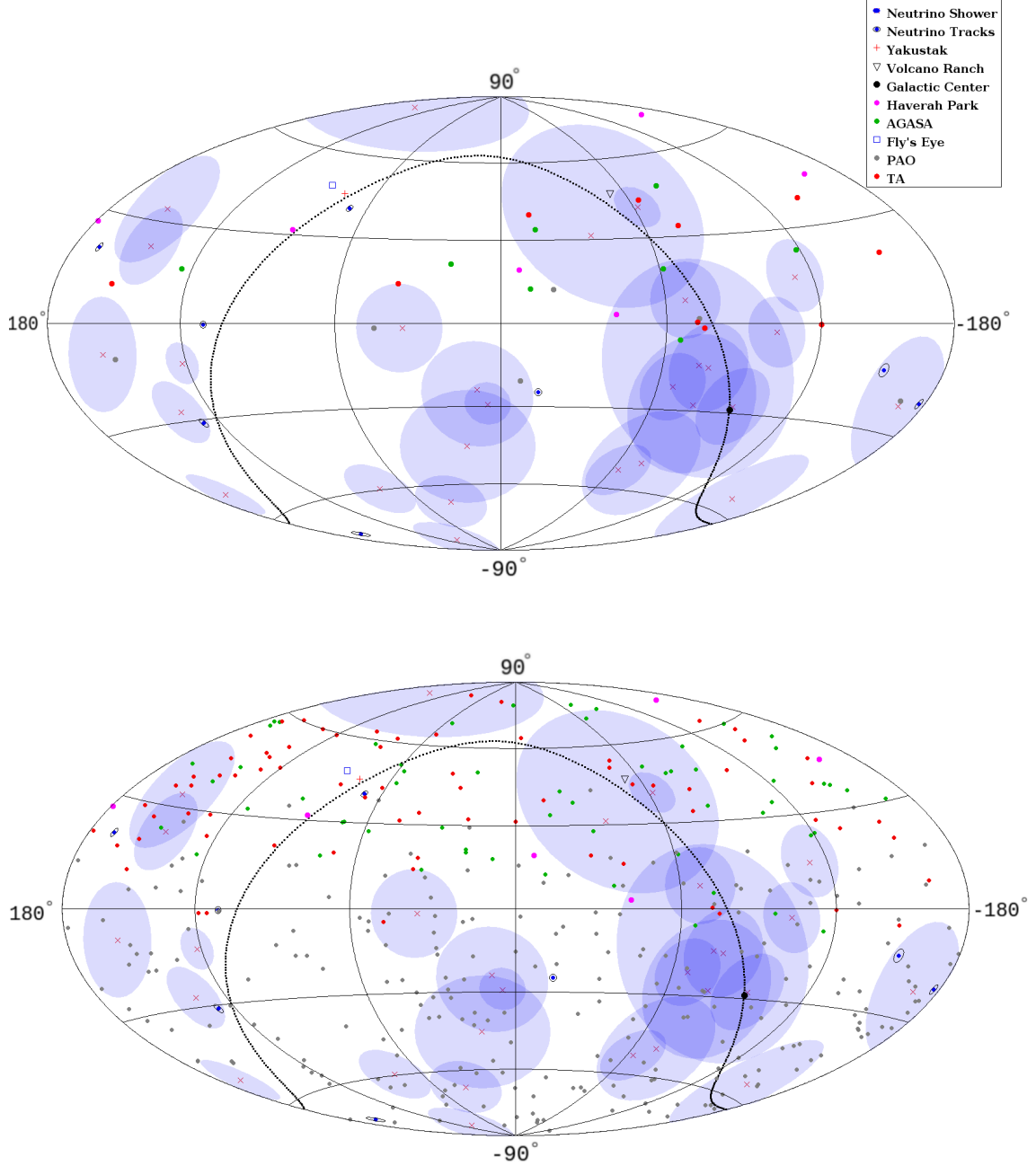


Figure 1. Sky maps of the IceCube > 30 TeV cosmic neutrino events with error circles and UHECR data in equatorial coordinates. The top panel shows UHECRs with energy ≥ 100 EeV and the bottom panel shows all available data with energy ≥ 40 EeV. The black dotted line is the Galactic plane.

We list in Table 1 all available UHECR data with energy ≥ 100 EeV. This includes 6 events from Haverah Park, 1 event from Yakutsk, 8 events from AGASA, 1 event from Volcano Ranch, the highest-energy (320 EeV) event from Fly's eye, 6 events from PAO and 10 events from TA. We use this list and sublists with PAO and TA data separately to study

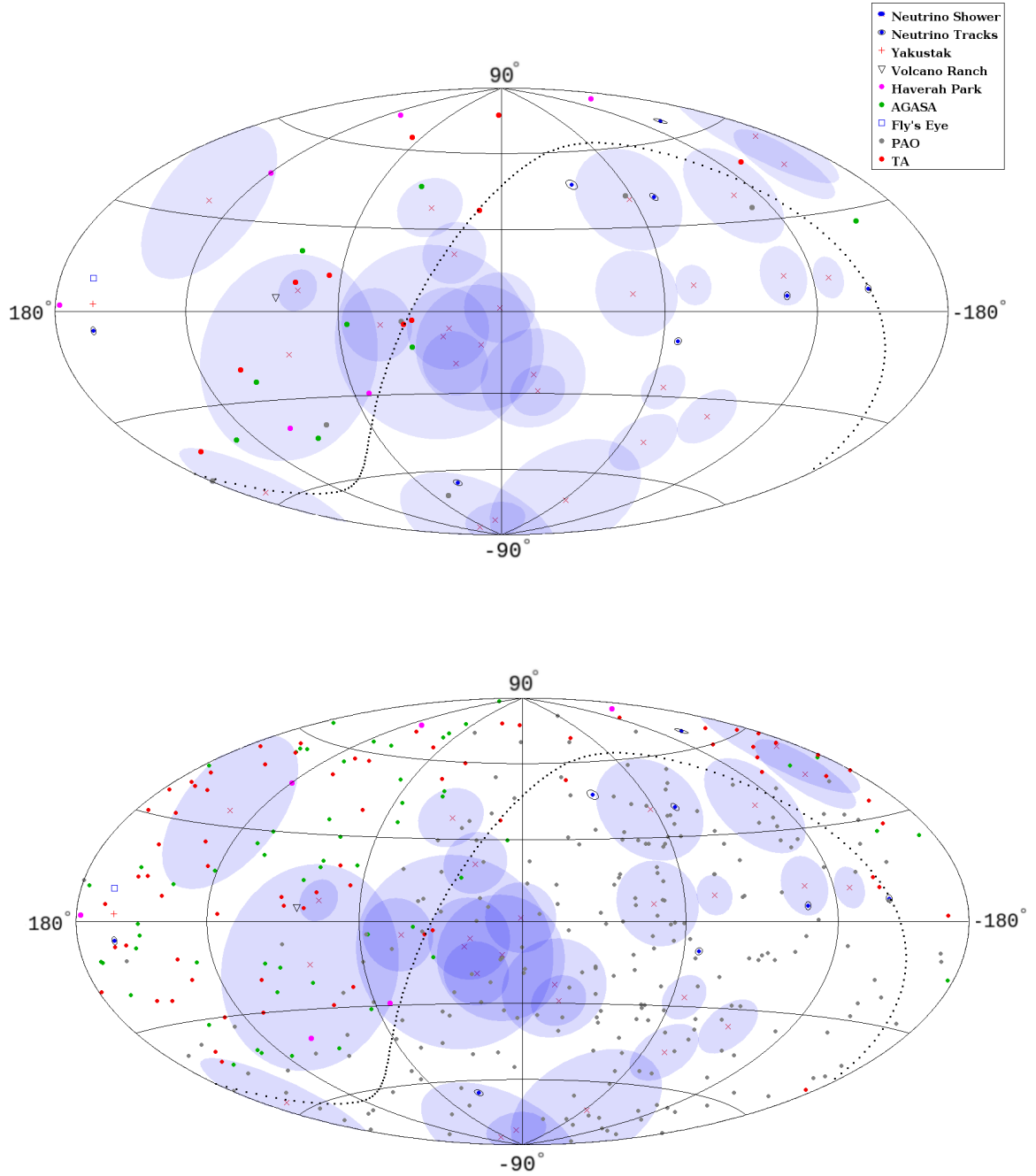


Figure 2. The same as Figure 1 but in Galactic coordinates.

correlation with cosmic neutrino events. In addition to ≥ 100 EeV data, we also explore energy-dependence of correlation by choosing different energy cuts, ≥ 80 EeV and ≥ 60 EeV, in UHECR data from the PAO, TA and AGASA. Above 80 EeV (60 EeV) there are 22 (136) UHECR events from PAO, 20 (60) from TA and 11 (22) from AGASA. We note that energy calibration across the experiments can vary by as much as $\sim 30\%$ (see, e.g., ref. [14]). We

Experiment	Reference	Energy (EeV)	RA (°)	Dec (°)
Haverah Park	[10]	101	201	71
Haverah Park	[10]	116	353	19
Haverah Park	[10]	126	179	27
Haverah Park	[10]	159	199	44
Haverah Park	[11]	123	318.3	3.0
Haverah Park	[11]	115	86.7	31.7
Yakutsk	[10]	110	75.2	45.5
AGASA	[12]	101	124.25	16.8
AGASA	[12]	213	18.75	21.1
AGASA	[12]	106	281.25	48.3
AGASA	[12]	144	241.5	23.0
AGASA	[12]	105	298.5	18.7
AGASA	[12]	150	294.5	-5.8
AGASA	[12]	120	349.0	12.3
AGASA	[12]	104	345.75	33.9
Volcano Ranch	[10]	135	306.7	46.8
Fly's eye	[10]	320	85.2 ± 0.5	$48.0^{+5.2}_{-6.3}$
Pierre Auger	[2]	108.2	45.6	-1.7
Pierre Auger	[2]	127.1	192.8	-21.2
Pierre Auger	[2]	111.8	352.6	-20.8
Pierre Auger	[2]	118.3	287.7	1.5
Pierre Auger	[2]	100.1	150.1	-10.3
Pierre Auger	[2]	118.3	340.6	12.0
Telescope Array	[3]	101.4	285.74	-1.69
Telescope Array	[3]	120.3	285.46	33.62
Telescope Array	[3]	139.0	152.27	11.10
Telescope Array	[3]	122.2	347.73	39.46
Telescope Array	[3]	154.3	239.85	-0.41
Telescope Array	[3]	162.2	205.08	20.05
Telescope Array	[3]	124.8	295.61	43.53
Telescope Array	[3]	135.5	288.30	0.34
Telescope Array	[3]	101.0	219.66	38.46
Telescope Array	[3]	106.8	37.59	13.89

Table 1. Available UHECR data with energy $\gtrsim 100$ EeV from various experiments.

discuss this issue in Sec. 4.2.

3 Statistical method and data analyses

To study correlation between cosmic neutrinos and UHECRs, we map the Right Ascension and Declination (RA, Dec) of the event directions into unit vectors on a sphere as

$$\hat{x} = (\sin \theta \cos \phi, \sin \theta \sin \phi, \cos \theta)^T,$$

where $\phi = RA$ and $\theta = \pi/2 - Dec$. Scalar product of the neutrino and UHECR vectors ($\hat{x}_{\text{neutrino}} \cdot \hat{x}_{\text{UHECR}}$) therefore is independent of the coordinate system. The angle between the

two vectors

$$\gamma = \cos^{-1}(\hat{x}_{\text{neutrino}} \cdot \hat{x}_{\text{UHECR}}), \quad (3.1)$$

is an invariant measure of the angular correlation between the neutrino and UHECR arrival directions [7, 8]. Following ref. [7] we use a statistic made from invariant γ for each neutrino direction \hat{x}_i and UHECR direction \hat{x}_j pair as

$$\delta\chi_i^2 = \min_j(\gamma_{ij}^2/\delta\gamma_i^2), \quad (3.2)$$

which is minimized for all j . Here $\delta\gamma_i$ is the 1- σ angular resolution of the neutrino events. We use the exact resolutions reported by the IceCube collaboration for each event [1].

A value $\delta\chi_i^2 \leq 1$ is considered a “good match” between the i -th neutrino and an UHECR arrival directions. We exploit distributions of all $\delta\chi_i^2$ statistic to study angular correlation between IceCube neutrino events and UHECR data. The distribution with observed data giving a number of “hits” or N_{hits} with $\delta\chi^2 \leq 1$ therefore forms a basis to claim correlation. Note that in case more than one UHECR directions are within the error circle of a neutrino event, the $\delta\chi^2$ value for UHECR closest to the neutrino direction is chosen in this method.

We estimate the significance of any correlation in data by comparing N_{hits} with corresponding number from null distributions. We construct two null distributions, in one case we randomize only the RA of UHECRs, keeping their Dec the same as in data; and in the second case we also randomize Dec according to the zenith-angle depended sky exposure of the UHECR experiments [36], affecting the declination distributions of UHECR data. We call these two null distributions as the *semi-isotropic null* and *exposure-corrected null*, respectively. The *semi-isotropic null* is a quick-way to check significance while the *exposure-corrected null* is accurate when information on particular experiments are available. In both cases we perform 100,000 realizations of drawing random numbers to assign new RA and Dec values for each event to construct $\delta\chi^2$ distributions in the same way as done with real data. We find that the two null distributions are in good agreement with each other in most cases.

We calculate statistical significance of correlation in real data or p -value (chance probability) using frequentists’ approach. We count the number of times we get a random data set that gives equal or more hits than the N_{hits} in real data within $\delta\chi^2 \leq 1$ bin. Dividing this number with the total number of random data sets generated (100,000) gives us the p -value. We cross-check this p -value by calculating the Poisson probability of obtaining N_{hits} within $\delta\chi^2 \leq 1$ bin given the corresponding average hits expected from the null distribution. These two chance probabilities are in good agreement.

4 Results

4.1 Correlations between neutrinos and UHECRs

We apply our statistical method separately to the PAO and TA data, to a combination of the both and to all available UHECR data above 100 EeV from all experiments (see Table 1). The results are shown in the histograms of Figure 3. The counts in the $0 \leq \delta\chi^2 \leq 1$ bins for the blue, filled histograms correspond to the number of correlated neutrino events with UHECRs. Counts in other bins are due to distant pairs of the neutrino events and UHECRs and are uninteresting for us. The counts for the red (green), open histogram in the same bins correspond to the expected number of correlated neutrino events from the *semi-isotropic null* (*exposure-corrected null*), after averaging over 100,000 simulated data sets with random UHECR positions. Both null distributions give similar results.

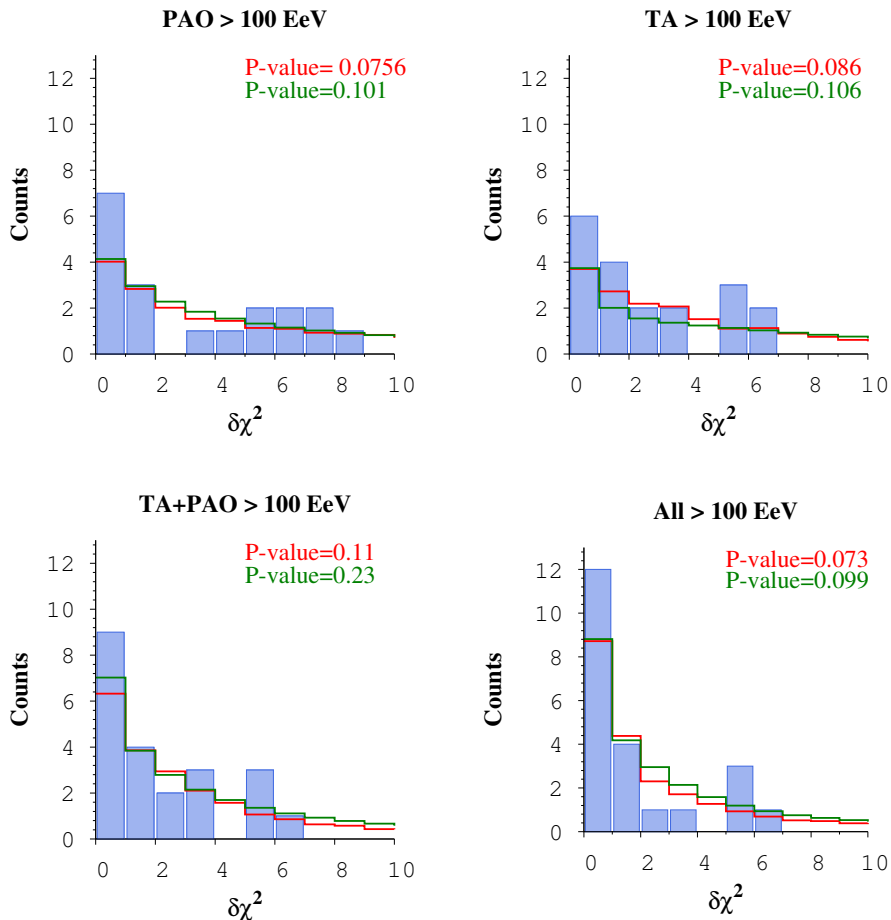


Figure 3. Distributions of $\delta\chi^2$ found in observed data (blue, filled histograms) and in simulated data corresponding to the *semi-isotropic null* (red, open histograms) and the *exposure-corrected null* (green, open histograms). The histograms have been truncated at $\delta\chi^2 = 10$ for better display. Significances (p -values) have been calculated for the $0 \leq \delta\chi^2 \leq 1$ bins.

Figure 3 also shows p -values or the probability of finding the correlated events ($0 \leq \delta\chi^2 \leq 1$) in observed data as a fluctuation of the randomly distributed UHECRs in the sky. The probability $1 - p \approx 90\%$ is the confidence level (CL) that the IceCube neutrino events and all available UHECR data with energy ≥ 100 EeV are correlated. A correlation with similar CL exists between the neutrino and PAO-only data sets and between the neutrino and TA-only data sets. The Poisson probability of obtaining $N_{\text{hits}} = 7$ in PAO data when 4 are expected from the *semi-isotropic null distribution* and $N_{\text{hits}} = 6$ in TA data with 3.8 expected from the same null distribution are ≈ 0.06 , in very good agreement with our p -values. Similarly, for the combined data set of all UHECRs > 100 EeV, $N_{\text{hits}} = 12$ when expected value is 8.8 corresponds to a Poisson probability of ≈ 0.07 , again in very good agreement with

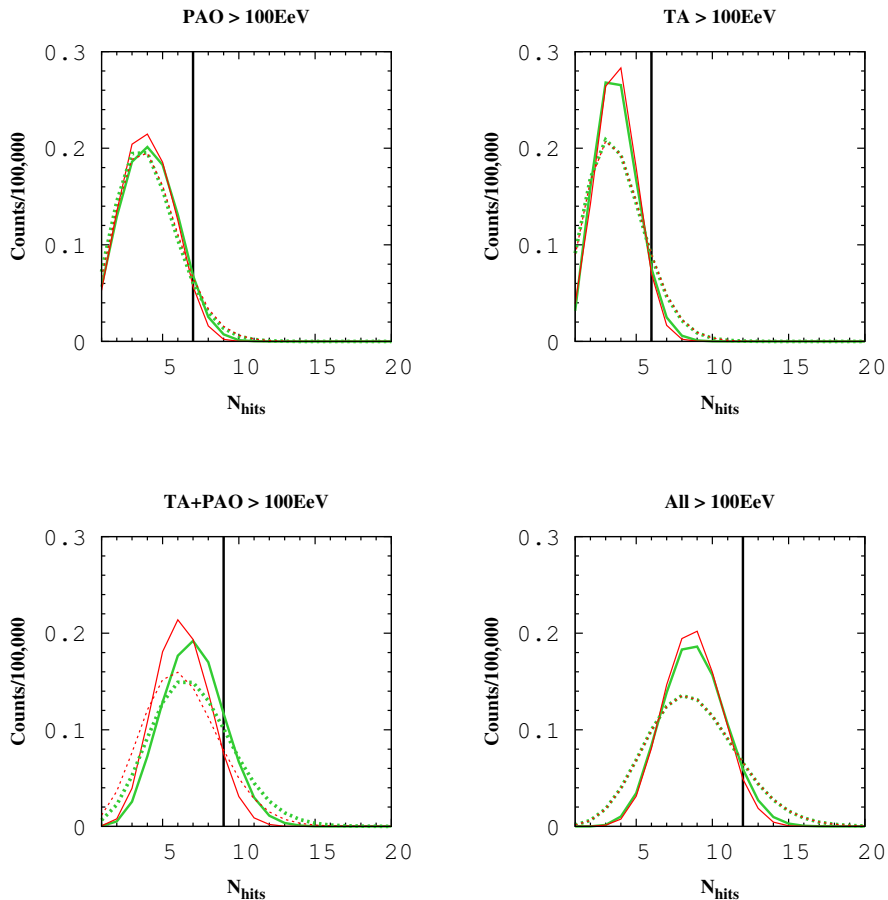


Figure 4. Comparisons between the N_{hits} distributions in the $\delta\chi^2 \leq 1$ bins of Fig. 3 obtained from the *semi-isotropic* (red solid lines) and *exposure-corrected* (green solid lines) null distributions. Also plotted are the Poisson distributions (dotted lines) for the average values of the respective null distributions in the $\delta\chi^2 \leq 1$ bins of Fig. 3. The vertical lines are the observed N_{hits} values in data.

our p -value.

We remind the readers that the counts in the $\delta\chi^2$ distributions with TA+PAO data is not the algebraic sum of the counts in the distributions with TA and PAO data separately. This is because our $\delta\chi^2$ statistic choose the nearest UHECR data point even if more than one are present within the error circle of a neutrino event. The same is true for distribution with all UHECRs. We list the correlated events in Table 2 against the neutrino event numbers in ref. [1]. Note that we list all UHECRs giving $\delta\chi^2 \leq 1$ in the table. There are 7 UHECRs which are correlated with 2 or more neutrino events. None of the correlated neutrinos are PeV neutrino events.

Figure 4 shows a comparison between the two null distributions for UHECRs with

ν event no. [1]	$\delta\chi^2$	Energy (EeV)	RA ($^\circ$)	Dec ($^\circ$)	Experiment
1	0.41	108.2	45.6	-1.7	PAO
	0.95	106.8	37.59	13.9	TA
2	0.97	150	294.5	-5.8	AGASA
11	0.10	100.1	150.1	-10.3	PAO
16	0.006	127.1	192.8	-21.2	PAO
17	0.77	144	241.5	23.0	AGASA
21	0.55	111.8	352.6	-20.8	PAO
24	0.78	101.4	285.74	-1.7	TA
	0.97	150	294.5	-5.8	AGASA
25	0.06	150	294.5	-5.8	AGASA
	0.07	101.4	285.74	-1.7	TA
	0.10	135.5	288.3	0.34	TA
	0.12	118.3	287.7	1.5	PAO
	0.58	105	298.5	18.7	AGASA
29	0.62	123	318.3	3	Haverah Park
	0.18	124.8	295.6	43.52	TA
31	0.35	101	201	71	Haverah Park
33	0.34	118.3	287.7	1.5	PAO
	0.40	135.5	288.3	0.34	TA
34	0.74	101.4	285.74	-1.7	TA
	0.84	105	298.5	18.7	AGASA
	0.20	104	345.75	34	AGASA
	0.22	135	306.7	46.8	Volcano Ranch
	0.25	122.2	347.7	39.46	TA
	0.34	118	340.6	12	PAO
	0.34	124.8	295.61	43.53	TA
	0.36	105	298.5	18.7	AGASA
	0.45	123	318.3	3	Haverah Park
	0.47	116	353	19	Haverah Park
34	0.50	120	349	12.3	AGASA
	0.55	120.3	285.5	33.62	TA
	0.71	134	281.25	48.3	AGASA

Table 2. IceCube cosmic neutrino events correlated with UHECRs above 100 EeV.

energy ≥ 100 EeV in Fig. 3 by using the N_{hits} within the $\delta\chi^2 \leq 1$ bin from simulations for both the null distributions. The two null distributions agree well in all cases except for the combined analysis of the TA and PAO data. A comparison with Poisson distribution with frequency for the corresponding cases are also shown. For PAO UHECRs >100 EeV the two null distributions follow the respective Poisson distributions but not for the other cases. The black vertical line represents the observed N_{hits} .

We do the same statistical analysis with UHECRs above 80 EeV. The results are shown in Figure 5. There are 6 new correlations in the PAO-only data. Only 10 is expected from our null distributions as compared to 13 total in data. This reduces correlation between the IceCube and PAO data to $\approx 84\% - 88\%$ CL. A list of UHECRs from the PAO correlated with the neutrino events is given in Table 3. Note that the 2 PeV neutrino event (event number

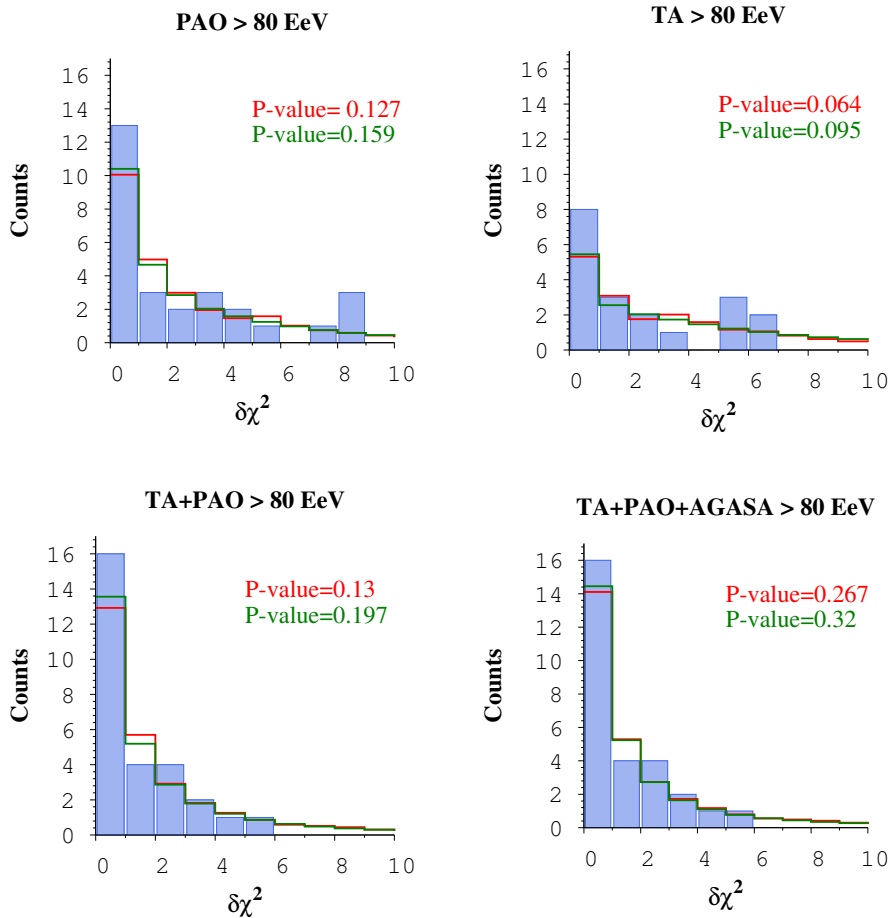


Figure 5. The same as in Figure 3 but for UHECRs with energy ≥ 80 EeV.

35), the highest observed energy so far [1], is now correlated with a 89.1 EeV PAO event. The other two neutrino events with energy ≈ 1 PeV each still remain uncorrelated with UHECRs with energy ≥ 80 EeV. There are 6 UHECRs in Table 3 which are correlated with more than one neutrino events. In particular an 82 EeV PAO event is correlated with 4 neutrino events.

Lowering the UHECR energy lower limit to 80 EeV adds 2 new correlated events in the case of TA-only data with a total of 8 as compared to ≈ 5.6 expected from both the null distributions, giving a CL of $\approx 90\%$. Combining the PAO and TA data results in similar significance as obtained from individual data sets. Combining the PAO, TA and AGASA data reduces the significance of correlation.

Further lowering the UHECR energy lower limit to 60 EeV gives no significant correlation between the IceCube cosmic neutrino data and UHECR data. Figure 6 shows that the number of correlated events in data is very similar to those expected from the null distributions in all cases. Such a loss of significance is expected when there is no real correlation between the

ν event no. [1]	$\delta\chi^2$	Energy (EeV)	RA ($^\circ$)	Dec ($^\circ$)
1	0.41	108.2	45.6	-1.7
2	0.002	80.9	283.7	-28.6
7	0.85	83.8	26.8	-24.8
11	0.10	100.1	150.1	-10.3
15	0.6	82.3	287.7	-64.9
16	0.006	127.1	192.8	-21.2
	0.52	84.7	199.7	-34.9
21	0.55	111.8	352.6	-20.8
21	0.6	83.8	26.8	-24.8
22	0.85	80.9	283.7	-28.6
24	0.77	80.9	283.7	-28.6
25	0.095	80.2	283.7	-28.6
	0.12	118.3	287.7	1.5
	0.61	82	299	19.4
	0.62	80.2	271.1	19.0
	0.67	81.4	308.8	16.1
33	0.34	82	287.7	1.5
	0.95	82	299	19.4
34	0.22	81.4	308.8	16.1
	0.34	82	299.	19.4
	0.34	118.3	340.6	12
	0.6	89	349.9	9.3
35	0.96	89.1	218.8	-70.8

Table 3. IceCube cosmic neutrino events correlated with UHECRs detected by PAO above 80 EeV.

data sets.

4.2 Energy calibrated events

As we noted earlier, energy calibration among different UHECR experiments is a widely-debated issue. If UHECR flux is uniform over the whole sky and each experiment measures the same primary particles’ energy then the number of UHECR events should be proportional to the exposures of the experiments. Therefore it is difficult, in particular, to reconcile the 10 TA events at > 100 EeV compared to the 6 from PAO, which has 20 times more exposure than TA. There are many energy rescaling procedure suggested among experiments (see, e.g., refs. [15–17]) to bring their respective measured fluxes close to each other, mostly at the “ankle” regime. Even these procedures cannot reconcile number of events, after exposure corrections, above 100 EeV among different experiments. It is plausible that the energy rescaling factors themselves are energy dependent, differing from the ankle regime to the GZK regime. Reconstructing such energy-dependent rescaling factors is beyond the scope of this paper. We hope the experimental collaborations will provide such factors in future.

To illustrate the energy rescaling effect on our correlation study, we adopt a recent procedure in ref. [15] which is based on a joint PAO and TA analysis of UHECRs from an overlapping region in the sky. We decrease the energies of the TA events by 25% but keep the energies of the PAO events unchanged [15]. So the number of UHECRs events above 100 EeV from TA is now 4, out of which only 2 correlates with the neutrino events in the

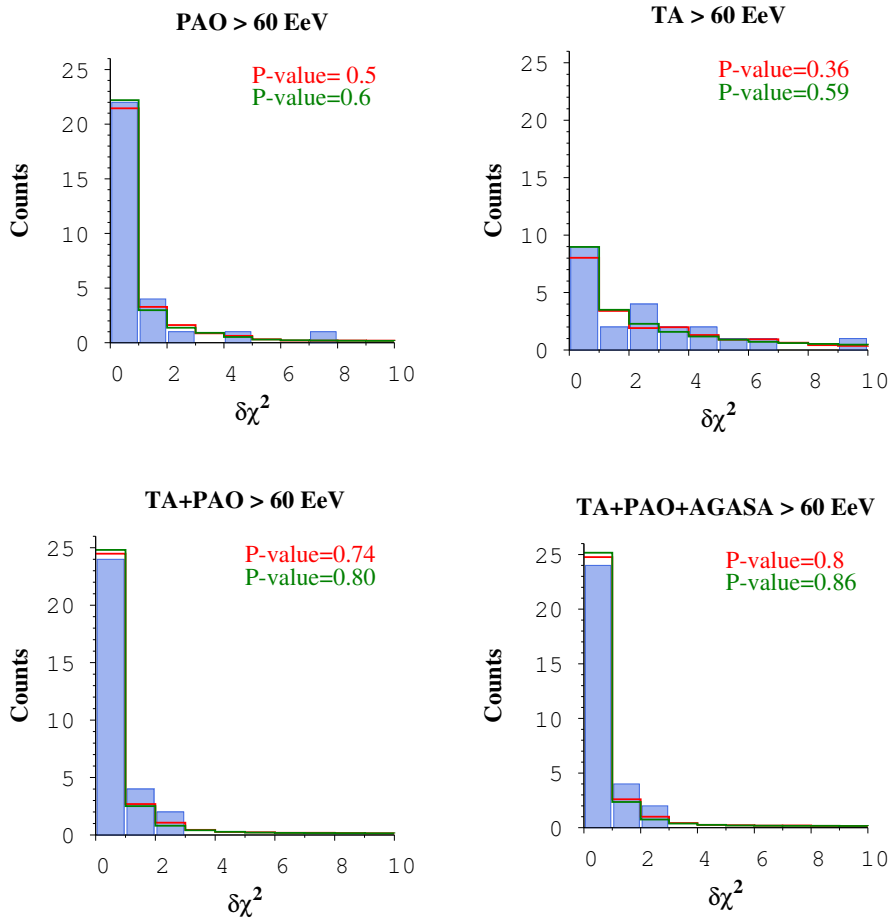


Figure 6. The same as in Figure 3 but for UHECRs with energy ≥ 60 EeV.

$\delta\chi^2 \leq 1$ bin (see Fig. 7). Interestingly, however, there are now 6 counts in the $1 \leq \delta\chi^2 \leq 2$ bin which corresponds to a Poisson probability of 0.0108 according to the *semi-isotropic null*. A combined analysis of the TA and PAO data considering the above energy rescaling, gives no significant correlation with neutrino data.

4.3 Astrophysical source search

We search for astrophysical source candidates for UHECRs which are correlated with IceCube cosmic neutrino events, assuming both are produced by the same sources. We use data from Tables 2 and 3 for this purpose. The experimental angular resolution of the UHECRs is of the order of 1° . However, Galactic and intergalactic magnetic field can deflect them by more than a few degrees from their source directions. The deflection angle in the intergalactic random

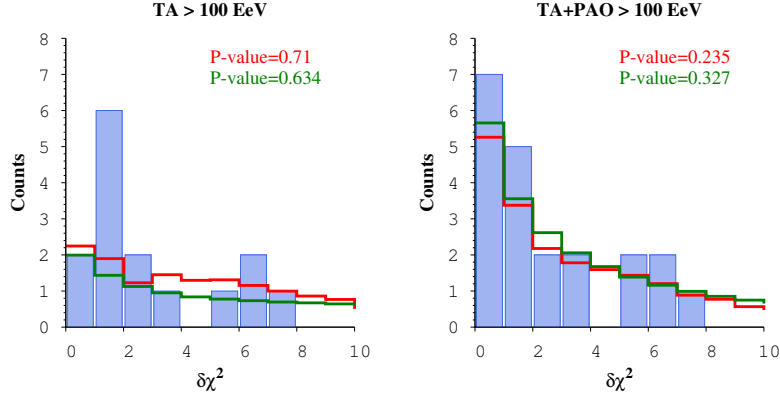


Figure 7. The same as in Figure 3 upper-right and bottom-left panels but the energies for the TA events have been reduced by 25% compared to the PAO events.

magnetic field [18] with strength B_{rdm} and coherence length λ_{coh} is

$$\delta\theta_{\text{IG}} \approx 1.1^\circ Z \left(\frac{E_{\text{cr}}}{100 \text{ EeV}} \right)^{-1} \left(\frac{B_{\text{rdm}}}{1 \text{ nG}} \right) \left(\frac{D}{200 \text{ Mpc}} \right)^{1/2} \left(\frac{\lambda_{\text{coh}}}{100 \text{ kpc}} \right)^{1/2} \quad (4.1)$$

where Z and E_{cr} are the charge and energy of the UHECR and D is the distance to the source. The deflection angle in a small-scale Galactic random magnetic field, using Eq. (4.1) with $B_{\text{rdm}} = 1\mu\text{G}$, $\lambda_{\text{coh}} = 100 \text{ pc}$ is much smaller, $\delta\theta_{\text{G}} \approx 0.2^\circ Z$, for $E_{\text{cr}} = 100 \text{ EeV}$ and $D = 10 \text{ kpc}$. However, the deflection angle in the large-scale regular component of the Galactic magnetic field in the disk and in the halo can be larger, $\sim 1^\circ\text{--}3^\circ$ [19, 20]. Hereafter we assume that UHECRs with energy $\geq 80 \text{ EeV}$ are dominantly protons¹. We also chose a conservative source search region of 3° around the directions of UHECRs which are correlated with cosmic neutrino events.

We also limit our source search within a comoving volume with its radius set by the GZK effect of $p_{\text{UHECR}} + \gamma_{\text{CMB}}$ interactions and corresponding energy losses by UHECR protons [5, 6]. A crude estimate of the mean-free-path for this interaction can be obtained from the number density of CMB photons with 2.73 K temperature in the local universe, which is

$$\epsilon n(\epsilon) = \frac{1.32 \times 10^4 (\epsilon/\text{meV})^3}{\exp[4.25(\epsilon/\text{meV})] - 1} \text{ cm}^{-3}. \quad (4.2)$$

Thus the number density is 244 cm^{-3} at the peak photon energy $\epsilon = 2.82k_B(2.73 \text{ K}) = 0.66 \text{ meV}$, where $k_B = 8.62 \times 10^{-5} \text{ eV K}^{-1}$ is the Boltzmann constant. A parametrization of the UHECR proton's mean-free-path, using delta function approximation of the $p\gamma$ cross section, is given by

$$\lambda_p \approx 245.76 \left(\frac{E_p}{100 \text{ EeV}} \right)^{-3} \exp \left[0.42 \left(\frac{E_p}{100 \text{ EeV}} \right) - 1 \right] \text{ Mpc}, \quad (4.3)$$

¹Note that the mass composition measurement by the PAO collaboration by using shower maxima, which favors heavy nuclei as primaries, is done up to an energy $\sim 60 \text{ EeV}$ only [22].

which reproduces results from numerical calculations with accurate treatment [21] within $\sim 10\%$ in the $\sim 60\text{--}200$ EeV range. For reference, $\lambda_p = 539, 247, 138$ and 26 Mpc at $E_p = 60, 80, 100$ and 200 EeV, respectively. We search for astrophysical sources within redshift $z = 0.06$, which corresponds to a luminosity distance $d_L = 270.4$ Mpc in Λ CDM cosmology with $H_0 = 69.6$ km s $^{-1}$ Mpc $^{-1}$, $\Omega_M = 0.286$ and $\Omega_\Lambda = 0.714$ [23]. The proper distance, $d_p = d_L/(1+z)^2 = 241$ Mpc, is similar to λ_p at 80 EeV.

We have used the *Swift*-BAT 70 month X-ray source catalog [24] to search for astrophysical sources which are correlated with UHECR and cosmic neutrino events. In 70 months of observations, the catalog includes 1210 objects of which 503 objects are within redshift ≤ 0.06 . Out of these 503 X-ray selected objects at least 18 are simultaneously correlated with the neutrino events and UHECRs above 100 EeV, see Table 4. The correlated X-ray sources are all Seyfert (Sy) galaxies except ABELL 2319 which is a galaxy cluster (GC). The X-ray luminosity of these sources vary between $L_X \approx 10^{43}\text{--}10^{45}$ erg s $^{-1}$, with Cygnus A the most luminous of all. Note that the PAO collaboration has also found an anisotropy at $\sim 98.6\%$ CL in UHECRs with energy ≥ 58 EeV and within $\sim 18^\circ$ circles around the AGNs in *Swift*-BAT catalog [24] at distance ≤ 130 Mpc and X-ray luminosity $L_X \gtrsim 10^{44}$ erg s $^{-1}$ [2]. Our list in Table 4 includes NGC 1142 which is also one of the five sources that dominantly contribute to the anisotropy found in the PAO data [2].

In another correlated source search we have used bright extragalactic radio sources with flux density ≥ 1 Jy at 5 MHz from the Kühr catalog [25]. It has 61 sources within known redshift ≤ 0.06 . Only 3 sources from this catalog are correlated simultaneously with IceCube neutrinos and UHECRs above 100 EeV, see Table 4. Two of these sources are Seyfert galaxies and the third one is a galaxy cluster. There are two common sources, that are correlated with both neutrinos and UHECRs, between the *Swift*-BAT and Kühr catalogs. These are NGC 1068 and PKS 2331-240. Both of them are Seyfert galaxies.

We have also searched the first AGN catalog (1LAC) published by the *Fermi*-LAT collaboration [26] for possible correlations with neutrino and UHECR arrival directions but did not find any.

It is interesting note that the cosmic neutrino events (nos. 2, 12, 14, 15 and 36) which are strongly correlated with the Fermi Bubbles² [27, 28], except for event no. 2, do not appear in Table 4. This could be a hint to possible extragalactic [29] and Galactic [30] components in the neutrino event data.

4.4 Neutrino and UHECR luminosities for correlated events

After searching for astrophysical sources correlated with both IceCube cosmic neutrino events and UHECRs, we calculate their corresponding fluxes required to produce observed events. First, we describe our point-source neutrino flux calculation method. We assume a power-law flux of the following form

$$J_{\nu\alpha}(E_\nu) = A_{\nu\alpha} \left(\frac{E_\nu}{100 \text{ TeV}} \right)^{-\kappa}, \quad (4.4)$$

which is the same for all 3 flavors: $\alpha = e, \mu, \tau$. We estimate the normalization factor from the number of neutrinos events N_ν of any flavor³ as

$$A_{\nu\alpha} = \frac{1}{3} \frac{N_\nu}{T \sum_\alpha \int_{E_{\nu 1}}^{E_{\nu 2}} dE_\nu A_{\text{eff},\alpha}(E_\nu) \left(\frac{E_\nu}{100 \text{ TeV}} \right)^{-\kappa}}, \quad (4.5)$$

²The centers of the error circles within the Fermi bubbles' contours

³Here we tacitly assume that flavor identification is not efficient.

Neutrino Event #	UHECR			<i>Swift</i> X-ray Source Catalog [24]		
	RA	Dec	Experiment	Name	z	Type
1	45.6	−1.7	PAO	NGC 1142	0.0289	Sy2
				NGC 1194	0.0136	Sy1
				MCG +00-09-042	0.0238	Sy2
				NGC 1068	0.0038	Sy2
11	150.1	−10.3	PAO	2MASX J10084862-0954510	0.0573	Sy1.8
17	241.5	23	AGASA	2MASX J16311554+2352577	0.0590	Sy2
29, 34	295.6	43.52	TA	2MASX J19471938+4449425	0.0539	Sy2
				ABELL 2319	0.0557	GC
				Cygnus A	0.0561	Sy2
21	352.6	−20.2	PAO	PKS 2331-240	0.0477	Sy2
2, 24, 25	294.5	−5.8	AGASA	2MASX J19373299-0613046	0.0103	Sy1.5
				34	340.6	12
	349.0	12.3	AGASA	MCG +02-57-002	0.0290	Sy1.5
				UGC 12237	0.0283	Sy2
				NGC 7479	0.0079	Sy2/Liner
				2MASX J23272195+1524375	0.0457	Sy1
	352.6	−20.2	Haverah Park	NGC 7469	0.0163	Sy1.2
NGC 7679				0.0171	Sy2	

Neutrino Event #	UHECR			Kühr Radio Source Catalog [25]		
	RA	Dec	Experiment	Name	z	Type
1	45.6	−1.7	PAO	NGC 1068	0.0038	Sy2
21	352.6	−20.8	PAO	PKS 2331-240	0.0477	Sy2
34	340.6	12	PAO	NGC 7385	0.0255	GC

Table 4. Sources correlated with UHECRs and neutrino events simultaneously.

where T is IceCube lifetime and $A_{\text{eff},\alpha}$ is effective area for different flavors. We use $T = 988$ days for IceCube 3-year data release [1] as in our correlation analysis and the following parametrization, correct within $\sim 10\%$ uncertainty, of the effective areas [31]

$$\begin{aligned}
A_{\text{eff},e} &= \begin{cases} [1.26 \times 10^{-5} (E_\nu/\text{TeV})^{2.64} - 0.017] \text{ m}^2, & 25 \text{ TeV} < E_\nu < 100 \text{ TeV} \\ [0.459 (E_\nu/\text{TeV})^{0.5} - 1.109] \text{ m}^2, & E_\nu > 100 \text{ TeV} \end{cases} \quad (4.6) \\
A_{\text{eff},\mu} &= \begin{cases} [3.6 \times 10^{-6} (E_\nu/\text{TeV})^{2.64} - 0.0142] \text{ m}^2, & 25 \text{ TeV} < E_\nu < 100 \text{ TeV} \\ [0.389 (E_\nu/\text{TeV})^{0.5} - 1.868] \text{ m}^2, & E_\nu > 100 \text{ TeV} \end{cases} \\
A_{\text{eff},\tau} &= \begin{cases} [7.267 \times 10^{-6} (E_\nu/\text{TeV})^{2.64} - 0.0175] \text{ m}^2, & 25 \text{ TeV} < E_\nu < 100 \text{ TeV} \\ [0.5069 (E_\nu/\text{TeV})^{0.5} - 3.092] \text{ m}^2, & E_\nu > 100 \text{ TeV}. \end{cases}
\end{aligned}$$

For the limits of the integral in Eq. (4.5) we set $E_{\nu 1} = 25$ TeV and $E_{\nu 2} = 2.2$ PeV, reflecting uncertainty in energy estimate reported by the IceCube collaboration [1].

We use neutrino flux to calculate neutrino luminosity of the corresponding source as

$$L_{\nu} = 4\pi d_L^2 \sum_{\alpha} \int_{E_{\nu 1}(1+z)}^{E_{\nu 2}(1+z)} dE_{\nu} E_{\nu} J_{\nu, \alpha}(E_{\nu}). \quad (4.7)$$

These luminosities are listed in Table 5. We use two values of κ , the choice $\kappa = 2.3$ is motivated by fit to IceCube data assuming an isotropic distribution of events [1, 32] and the choice $\kappa = 2.1$ is motivated by the cosmic-ray spectrum expected from Fermi acceleration mechanisms. Note that $N_{\nu} = 3$ for 2MASX J19373299-0613046, $N_{\nu} = 2$ for 2MASX J19471938+4449425 and $N_{\nu} = 1$ for all other sources. Neutrino luminosities listed in Table 5 are within a factor 5 of the corresponding X-ray luminosities of the sources. For the radio sources, neutrino luminosity far exceeds the corresponding radio luminosity.

We also calculate UHECR flux from the observed events by using exposure for the respective experiments. We use a power-law form for the observed UHECR flux above 28.8 EeV break energy as [33]

$$J_{\text{uhecr}}(E_{\text{cr}}) = A_{\text{uhecr}} \left(\frac{E_{\text{cr}}}{\text{EeV}} \right)^{-4.3}; \quad E_{\text{cr}} \geq 28.8 \text{ EeV}, \quad (4.8)$$

and derive the normalization factor as

$$A_{\text{uhecr}} = \frac{N_{\text{uhecr}}}{\frac{\Xi \omega(\delta)}{\Omega} \int_{E_{\text{cr}1}}^{E_{\text{cr}2}} dE_{\text{cr}} \left(\frac{E_{\text{cr}}}{\text{EeV}} \right)^{-4.3}}. \quad (4.9)$$

Here Ξ is the total integrated exposure, as mentioned in ref. [34], Ω is the solid angle of the detector and $\omega(\delta)$ is the relative exposure for particular declination angle δ . For reference, we use for PAO, $\Xi_{\text{PAO}} = 66,000 \text{ km}^2 \text{ yr sr}$ and $\Omega_{\text{PAO}} = 1.65\pi \text{ sr}$ [2]; for TA, $\Xi_{\text{TA}} = 3,690 \text{ km}^2 \text{ yr sr}$ and $\Omega_{\text{TA}} = 0.85\pi \text{ sr}$ [3]; for AGASA, $\Xi_{\text{AGASA}} = 1,000 \text{ km}^2 \text{ yr sr}$ and $\Omega_{\text{AGASA}} = 0.59\pi \text{ sr}$ [35]. We do not use the Haverah Park event that is correlated with a neutrino event. We calculate $\omega(\delta)$ from ref. [36] but adapt it for different experiments by using their respective geographical locations and zenith angle ranges. For the lower and upper limits of integration in Eq. (4.9), we use $E_{\text{cr}1} = 80 \text{ EeV}$ and $E_{\text{cr}2} = 180 \text{ EeV}$, allowing a 20% uncertainty for the 100 EeV threshold energy used to search correlation and 150 EeV maximum energy found for a UHECR correlated with a neutrino event and a source (see Table 2).

In order to calculate cosmic-ray⁴ luminosity of the sources, first we note that if cosmic neutrinos detected by IceCube are coming from the same source that are correlated with UHECRs, then the cosmic-ray flux in Eq. (4.8) needs to be extrapolated down to ~ 500 TeV which is required to produce ~ 30 TeV neutrinos. Second, the flux in Eq. (4.8) needs to be corrected for GZK suppression above ~ 40 EeV. Given a cosmic-ray proton luminosity L_{cr} between the generation energies $E'_{\text{cr}1} = 500 \text{ TeV}$ and $E'_{\text{cr}2} = 180 \text{ EeV}$ with $\propto E'^{-\kappa}$ spectrum in a source at redshift z , the cosmic-ray flux on the Earth is [37, 38]

$$J_{\text{cr}}(E_{\text{cr}}) = \frac{L_{\text{cr}}(1+z)}{4\pi d_L^2} \frac{(\kappa - 2)(E'_{\text{cr}1} E'_{\text{cr}2})^{\kappa - 2}}{E'^{\kappa - 2}_{\text{cr}2} - E'^{\kappa - 2}_{\text{cr}1}} E'^{-\kappa}_{\text{cr}} \left(\frac{dE'_{\text{cr}}}{dE_{\text{cr}}} \right). \quad (4.10)$$

The cosmic-ray energy at the source and on the Earth are related through various energy losses [37]. Following ref. [38] we have plotted cosmic-ray flux in Fig. 8 using Eq. (4.10) for

⁴We assume they are dominantly protons.

Source name	L_X (10^{44} erg/s) / L_R (10^{41} erg/s)	L_ν (10^{44} erg/s)		L_{cr} (10^{44} erg/s)	
		$\kappa = 2.1$	$= 2.3$	$\kappa = 2.1$	$= 2.3$
NGC 1142	1.58/0.012(74 GHz)	0.95	1.0	0.7	5.4
NGC 1194	0.12/0.00012(1.4 GHz)	0.2	0.2	0.04	0.2
MCG +00-09-042	0.17/0.0043(1.4 GHz)	0.64	0.71	0.3	2.1
NGC 1068	0.031/0.0034(31.4 GHz)	0.016	0.017	0.001	0.007
2MASX J10084862-0954510	1.04/0.0028(1.4 GHz)	3.9	4.32	44	578
2MASX J16311554+2352577	0.79/0.0048(1.4 GHz)	4.1	4.6	1600	22000
2MASX J19471938+4449425	1.66/0.0045(1.4 GHz)	6.8	7.6	211	26000
ABELL 2319	1.78/0.0046(1.4 GHz)	3.7	4.1	270	3500
Cygnus A	11.2/314(14.7 GHz)	3.7	4.1	290	3700
PKS 2331-240	0.81/1.32(31.4 GHz)	2.6	2.9	9.5	102
2MASX J19373299-0613046	0.055/0.0012(1.4 GHz)	0.24	0.26	1.3	7.3
MCG +01-57-016	0.23/0.0026(1.4 GHz)	0.71	0.78	0.5	3.6
MCG +02-57-002	0.25/0.00084(1.4 GHz)	0.95	1.1	1.0	7.5
UGC 12237	0.23/0.0011(1.4 GHz)	0.91	1.	0.9	6.6
NGC 7479	0.029/0.04(22 GHz)	0.07	0.08	0.3	1.4
2MASX J23272195+1524375	0.51/0.24(1.4 GHz)	2.4	2.7	280	2900
NGC 7469	0.4/0.0056(365 MHz)	0.3	0.3	2.2	14
NGC 7679	0.1/0.00033(1.4 GHz)	-	-	-	-
NGC 1068	0.031/0.0034(31.4 GHz)	0.016	0.017	0.001	0.007
PKS 2331-240	0.81/1.32(31.4 GHz)	2.6	2.9	9.5	102
NGC 7385	- /0.17(31.4 GHz)	0.7	0.8	0.5	4.0

Table 5. Neutrino (25 TeV–2.2 PeV) and cosmic-ray (500 TeV–180 EeV) luminosities required for the correlated sources in Table 4 to produce observed data. Also listed are *Swift*-BAT X-ray luminosity [24] radio luminosity for these sources, with corresponding radio frequencies in parentheses.

$L_{\text{cr}} = 10^{44}$ erg s $^{-1}$ and for various redshift in the range $0.01 \leq z \leq 0.06$. We have also used two different values for κ as we did for neutrino flux calculation.

Figure 8 provides a map to estimate cosmic-ray luminosity of the sources listed in Table 4 which are correlated with UHECR and neutrino events. The UHECR flux in Eq. (4.8), calculated from data, corresponds to a point in Fig. 8 at $E_{\text{cr}} \approx 80$ EeV. We estimate the source luminosity L_{cr} by equating this flux to the expected flux in Eq. (4.10) at 80 EeV for the redshift of a given source. These luminosities are listed in Table 5. Note that except for NGC 1068 ($z = 0.0038$), NGC 1194 ($z = 0.0136$) and MCG +00-09-042 ($z = 0.0238$) the cosmic-ray luminosity with $\kappa = 2.1$ is comparable or higher than the neutrino luminosity for

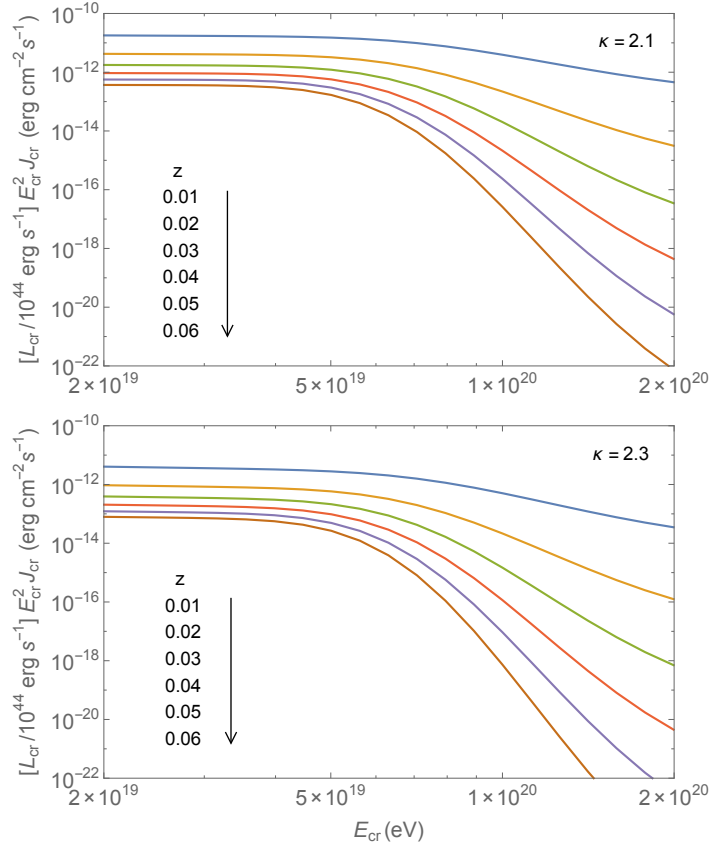


Figure 8. Expected UHECR flux on the Earth from sources at different redshift $0.01 \leq z \leq 0.06$ but with fixed luminosity $L_p = 10^{44} \text{ erg s}^{-1}$ in the 500 TeV to 200 EeV range.

all sources. The cosmic-ray luminosity exceeds the X-ray or radio luminosities for all sources except for NGC 1142 and NGC 1194, in case $\kappa = 2.1$.

5 Discussion and Outlook

We have investigated whether the arrival directions of cosmic neutrinos, detected by IceCube [1], with energy $\sim 30 \text{ TeV} - 2 \text{ PeV}$ are correlated with the arrival directions of UHECRs with energy $\gtrsim 100 \text{ EeV}$. In order to test correlation we have used an invariant statistic, called the minimum $\delta\chi^2$ [7], which is constructed from the angle between two unit vectors corresponding to the directions of the neutrino events and UHECRs, and weighted by the angular resolutions of the neutrino events. We have evaluated the significance of any correlation by using Monte Carlo simulations of randomly generated UHECR directions and comparing with data. We found that IceCube cosmic neutrinos are correlated with UHECRs with energy $\geq 100 \text{ EeV}$ with significance at 90% CL. The significance, however, decreases with decreasing energy of UHECRs, leaving no correlation at an energy threshold of 60 EeV. To take into account trial factor, since we searched for correlation with $N_{\text{trial}} = 3$ UHECR energy thresholds, we calculate post-trial p -value as $p_{\text{post-trial}} = 1 - (1 - p_{\text{signal}})^{1/N_{\text{trial}}} = 0.27$, with $p_{\text{signal}} = 0.1$ that we found in data.

We have searched for astrophysical sources in the *Swift*-BAT X-ray catalog [24], the Kühr radio source catalog [25] and *Fermi*-LAT 1LAC AGN catalog [26] within 3° error circles

of the ≥ 100 EeV UHECRs which are correlated with cosmic neutrino events, assuming the UHECRs are protons. We made a cut in redshift, $z \leq 0.06$, while searching for sources in the catalogs. This corresponds to a proper distance of 241 Mpc, similar to the mean-free-path of an 80 EeV proton in the CMB. The choice of 3° error circle is motivated by deflection of UHECR protons in the intergalactic and Galactic magnetic fields. We found that 18 sources from the *Swift*-BAT X-ray catalog and 3 sources from the Kühr radio source catalog are within 3° error circles of the UHECRs that are correlated with cosmic neutrinos. Except for ABELL 2319 and NGC 7385 which are galaxy clusters, the rest of the sources are Seyfert galaxies with Cygnus A being the most well known. Our finding is consistent with that of the PAO collaboration who found significant correlation between UHECR arrival directions and Seyfert galaxies in the *Swift*-BAT X-ray catalog [2]. We did not find any source from the *Fermi*-LAT 1LAC AGN catalog fitting our search criteria.

Estimates of the neutrino and UHECR fluxes for the correlated events were used to calculate corresponding 25 TeV–2.2 PeV neutrino luminosity and 500 TeV–180 EeV cosmic-ray luminosity under the hypothesis that both originated from the sources we found in the *Swift*-BAT and Kühr catalogs. The neutrino luminosities are of the same order as the X-ray luminosities of the sources. The cosmic-ray luminosities, depending on the source spectrum, are comparable or higher than both the neutrino and X-ray luminosities. Comparison between the nonthermal X-ray luminosity with the cosmic-ray or neutrino luminosity gives a possibility that the energy in X-ray producing electrons can be compared to that of cosmic-ray protons, both accelerated at the sources.

Acceleration of UHECRs near the central black holes of AGNs was proposed over 20 years ago [39, 40]. Interactions of these UHECRs with UV and X-ray photons could produce high-energy neutrinos [39, 41]. Seyfert galaxies are radio-quiet AGNs and do not have strong jets, although parsec scale jets in them have been observed in the last decade [42–44]. Collisions between blobs in this jet and formation of shocks may lead to acceleration of protons to an energy at least up to 10^{18} eV, with subsequent photomeson interactions producing high-energy neutrinos [45]. Acceleration of heavy nuclei and subsequent gamma-ray and neutrino production in radio-quiet AGNs have also been discussed [46]. Predictions have also been made for GeV–TeV gamma-ray emission from UHECR interactions in Cygnus A [47], which is also a powerful radio galaxy (3C 405).

If a fraction η_X of the X-ray luminosity, $L_X = 10^{44} L_{44}$ erg s $^{-1}$, of the Seyfert galaxies is nonthermal then one can estimate the energy density in magnetic field in the X-ray emitting region as $B^2/8\pi = \eta_X L_X/4\pi R^2 c$. Using $R \approx 10^{14} R_{14}$ cm, 3 times the Schwarzschild radius of a black hole of mass $M_{\text{bh}} = 10^8 M_\odot$, the magnetic field is $B = 10^3 (\eta_X L_{44})^{1/2} R_{14}^{-1}$ G. Assuming protons are accelerated in the same region, their maximum energy can be $E_{\text{max}} = eBR = 2.4 \times 10^{19} (\eta_X L_{44})^{1/2}$ eV. This is problematic for the X-ray luminosities of Seyfert galaxies in Table 5, which are correlated with ≥ 100 EeV cosmic rays, and the magnetic energy density must exceed the nonthermal X-ray energy density by a factor $\gtrsim 10$ for proton acceleration to $\sim 10^{20}$ eV. This additional energy could be accommodated if a sizable fraction of the Eddington luminosity, $L_{\text{Edd}} = 1.3 \times 10^{46} (M_{\text{bh}}/10^8 M_\odot)$ erg s $^{-1}$, could be converted to magnetic energy. The required cosmic-ray luminosities ($\kappa = 2.1$) in Table 5 for Seyfert galaxies are above the Eddington luminosity for 2MASX J16311554+2352577, 2MASX J19471938+4449425, 2MASX J23272195+1524375. In case of Cygnus A, M_{bh} and L_{Edd} are an order of magnitude larger. The $\kappa = 2.3$ cosmic-ray luminosities are more problematic. The opacity for photomeson ($p\gamma$) interactions with $\epsilon_X = 1$ keV X-ray photons and the subsequent $\gtrsim 15$ TeV neutrino production opacity is $\tau_{p\gamma} \approx 1 L_{44} R_{14}^{-1} (\epsilon_X/1 \text{ keV})^{-1}$.

A hint of correlation that we found between the IceCube cosmic neutrino events and UHECRs with energy ≥ 100 EeV should be investigated further by the experimental collaborations. Establishing a concrete correlation will be a ground-breaking discovery. Also a future extension of IceCube to increase its sensitivity in the > 1 PeV range will be very useful to probe the cosmic neutrino spectrum and if there is a cutoff in the spectrum. A cutoff in the spectrum is not natural at the PeV scale if the same sources produce ≥ 100 EeV cosmic rays and neutrinos. Whether the weak AGNs, which are plentiful in the nearby universe, are the sources of UHECRs and neutrinos or not is a question that will continued to be debated and investigated in the years to come.

Acknowledgments

We thank Paul Sommers for useful comments. We also thank an anonymous referee for helpful suggestions to improve this work. This work was supported in part by the National Research Foundation (South Africa) grants nos. 87823 (CPRR) and 91802 (Blue Skies). This research has made use of the VizieR catalog access tool, CDS, Strasbourg, France. The original description of the VizieR service was published in A&AS 143, 23.

References

- [1] M. G. Aartsen *et al.* [IceCube Collaboration], Phys. Rev. Lett. **113**, 101101 (2014) [arXiv:1405.5303 [astro-ph.HE]].
- [2] A. Aab *et al.* [Pierre Auger Collaboration], arXiv:1411.6111 [astro-ph.HE].
- [3] R. U. Abbasi *et al.* [Telescope Array Collaboration], Astrophys. J. **790**, L21 (2014) [arXiv:1404.5890 [astro-ph.HE]].
- [4] P. Sommers and S. Westerhoff, New J. Phys. **11**, 055004 (2009) [arXiv:0802.1267 [astro-ph]].
- [5] K. Greisen, Phys. Rev. Lett. **16**, 748 (1966).
- [6] G. T. Zatsepin and V. A. Kuzmin, JETP Lett. **4**, 78 (1966) [Pisma Zh. Eksp. Teor. Fiz. **4**, 114 (1966)].
- [7] A. Virmani, S. Bhattacharya, P. Jain, S. Razzaque, J. P. Ralston and D. W. McKay, Astropart. Phys. **17**, 489 (2002) [astro-ph/0010235].
- [8] S. Razzaque and J. P. Ralston, JCAP **0307**, 007 (2003) [astro-ph/0110045].
- [9] C. Bonifazi [Pierre Auger Collaboration], Nucl. Phys. Proc. Suppl. **190**, 20 (2009) [arXiv:0901.3138 [astro-ph.HE]].
- [10] M. Nagano and A. A. Watson, Rev. Mod. Phys. **72**, 689 (2000).
- [11] M. Ave, J. A. Hinton, R. A. Vazquez, A. A. Watson and E. Zas, Phys. Rev. Lett. **85**, 2244 (2000) [astro-ph/0007386].
- [12] M. Takeda, N. Hayashida, K. Honda, N. Inoue, K. Kadota, F. Kakimoto, K. Kamata and S. Kawaguchi *et al.*, Astrophys. J. **522**, 225 (1999) [astro-ph/9902239].
- [13] R. U. Abbasi, T. Abu-Zayyad, M. Allen, J. F. Amman, G. Archbold, K. Belov, J. W. Belz and S. Y. BenZvi *et al.*, Astropart. Phys. **30**, 175 (2008) [arXiv:0804.0382 [astro-ph]].
- [14] J. Blumer, R. Engel and J. R. Horandel, Prog. Part. Nucl. Phys. **63**, 293 (2009) [arXiv:0904.0725 [astro-ph.HE]].
- [15] A. Aab *et al.* [Telescope Array and Pierre Auger Collaborations], Astrophys. J. **794**, no. 2, 172 (2014) [arXiv:1409.3128 [astro-ph.HE]].

- [16] B. R. Dawson *et al.* [Pierre Auger and Yakutsk and Telescope Array Collaborations], EPJ Web Conf. **53**, 01005 (2013) [arXiv:1306.6138 [astro-ph.HE]].
- [17] A. A. Ivanov, Astrophys. J. **712**, 746 (2010) [arXiv:1002.2472 [astro-ph.HE]].
- [18] E. Waxman and J. Miralda-Escude, Astrophys. J. **472**, L89 (1996) [astro-ph/9607059].
- [19] G. R. Farrar, R. Jansson, I. J. Feain and B. M. Gaensler, JCAP **1301**, 023 (2013) [arXiv:1211.7086 [astro-ph.HE]].
- [20] H. N. He, A. Kusenko, S. Nagataki, R. Z. Yang and Y. Z. Fan, arXiv:1411.5273 [astro-ph.HE].
- [21] T. Stanev, R. Engel, A. Mucke, R. J. Protheroe and J. P. Rachen, Phys. Rev. D **62**, 093005 (2000) [astro-ph/0003484].
- [22] A. Aab *et al.* [Pierre Auger Collaboration], arXiv:1307.5059 [astro-ph.HE].
- [23] E. L. Wright, Publ. Astron. Soc. Pac. **118**, 1711 (2006) [astro-ph/0609593].
- [24] W. H. Baumgartner, J. Tueller, C. B. Markwardt, G. K. Skinner, S. Barthelmy *et al.*, Astrophys. J. Supplement series **207**, 19 (2014) arXiv:1212.3336 [astro-ph.HE].
- [25] H. Kuhr, A. Witzel, I. I. K. Pauliny-Toth and U. Nauber, Astron. Astrophys. Suppl. Ser. **45**, 367-430 (1981)
- [26] A. A. Abdo *et al.* [Fermi-LAT Collaboration], Astrophys. J. **715**, 429 (2010) [arXiv:1002.0150 [astro-ph.HE]].
- [27] C. Lunardini, S. Razzaque, K. T. Theodoseou and L. Yang, Phys. Rev. D **90**, 023016 (2014) [arXiv:1311.7188 [astro-ph.HE]].
- [28] C. Lunardini, S. Razzaque and L. Yang, arXiv:1412.6240 [astro-ph.HE].
- [29] F. W. Stecker, Phys. Rev. D **88**, 047301 (2013) [arXiv:1305.7404 [astro-ph.HE]].
- [30] S. Razzaque, Phys. Rev. D **88**, 081302 (2013) [arXiv:1309.2756 [astro-ph.HE]].
- [31] M. Aartsen *et al.* (IceCube Collaboration), Science **342**, 1242856 (2013), arXiv:1311.5238 [astro-ph.HE].
- [32] L. A. Anchordoqui, H. Goldberg, M. H. Lynch, A. V. Olinto, T. C. Paul and T. J. Weiler, Phys. Rev. D **89**, no. 8, 083003 (2014) [arXiv:1306.5021 [astro-ph.HE]].
- [33] J. Abraham *et al.* [Pierre Auger Collaboration], Phys. Lett. B **685**, 239 (2010) [arXiv:1002.1975 [astro-ph.HE]].
- [34] A. Cuoco and S. Hannestad, Phys. Rev. D **78**, 023007 (2008) [arXiv:0712.1830 [astro-ph]].
- [35] N. Hayashida, K. Honda, N. Inoue, K. Kadota, F. Kakimoto, S. Kakizawa, K. Kamata and S. Kawaguchi *et al.*, astro-ph/0008102.
- [36] P. Sommers, Astropart. Phys. **14**, 271 (2001) [astro-ph/0004016].
- [37] V. Berezhinsky, A. Z. Gazizov and S. I. Grigorieva, Phys. Rev. D **74**, 043005 (2006) [hep-ph/0204357].
- [38] S. Razzaque, C. D. Dermer and J. D. Finke, Astrophys. J. **745**, 196 (2012) [arXiv:1110.0853 [astro-ph.HE]].
- [39] F. W. Stecker, C. Done, M.H. Salamon & P. Sommers, Phys. Rev. Lett. **66**, 2697 (1991).
- [40] R. J. Protheroe & A. P. Szabo, Phys. Rev. Lett. **69**, 2697 (1992).
- [41] A. P. Szabo and R. J. Protheroe, Astropart. Phys. **2**, 375 (1994) [astro-ph/9405020].
- [42] C. G. Mundell, J.M. Wrobel, A. Pedlar & J.F. Gallimore, Astrophys. J. **583**, 192 (2003).
- [43] J.F. Gallimore, S.A. Baum & C.P. O'Dea, Astrophys. J. **613**, 794 (2004).

- [44] E. Middelberg, I. Agudo, A.L. Roy & T.P. Krichbaum, *Mon. Not. R. Astron. Soc.* **377**, 731 (2007).
- [45] J. Alvarez-Muniz and P. Meszaros, *Phys. Rev. D* **70**, 123001 (2004) [astro-ph/0409034].
- [46] A. Pe'er, K. Murase and P. Meszaros, *Phys. Rev. D* **80**, 123018 (2009) [arXiv:0911.1776 [astro-ph.HE]].
- [47] A. Atoyan and C. D. Dermer, *Astrophys. J.* **687**, L75 (2008) [arXiv:0808.0161 [astro-ph]].